

The Brazilian Disc Test under a Non-Uniform Contact Pressure Along its Thickness

Mehdi Serati · Habib Alehossein ·
Nazife Erarslan

Received: date / Accepted: date

Keywords Analytical solution · Brazilian test (BTS) · Double Fourier series · Papkovitch-Neuber potentials · Tensile strength

List of Symbols

F	Applied force at failure in a Brazilian test
$I_m(\gamma_n r)$	The modified Bessel function of the first kind of order m and the non-negative argument $\gamma_n r$
$2L, r_0$	Thickness and radius of a Brazilian disc specimen
m, n, B_{mn}, D_{mn}	Constants
P	Total load per radial length applied on the lateral curved surface of a Brazilian disc
2α	Contact loading angle in a Brazilian disc
r, θ, z	Polar coordinates
x, y, z	Cartesian coordinates
σ_{rr}	Radial stress components in cylindrical coordinates
$\phi_{(r,\theta,z)}, \psi_{(\psi_r, \psi_\theta, \psi_z)}$	Harmonic scalar and harmonic vector potentials in cylindrical coordinates, respectively

M. Serati
The University of Queensland, School of Civil Engineering, Brisbane, QLD 4072, Australia
Tel.: +61-7-33653520
E-mail: m.serati@uq.edu.au

H. Alehossein
University of Southern Queensland, School of Civil Engineering and Surveying, West St,
Toowoomba, QLD 4350, Australia

N. Erarslan
The University of Queensland, School of Civil Engineering, Brisbane, QLD 4072, Australia

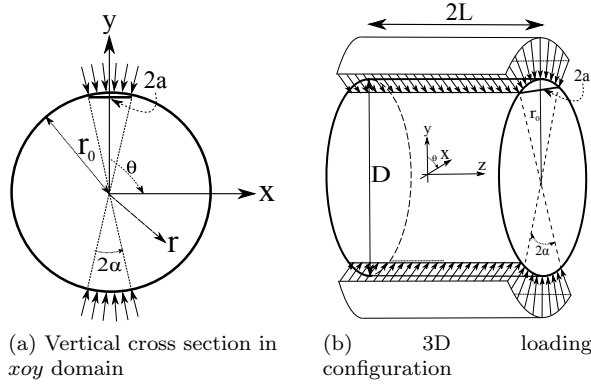


Fig. 1 Cross sections of a standard Brazilian disc subjected to diametrically opposite radial loads

1 Introduction

The indirect Brazilian Tensile Strength (BTS) test, with a long history of applications in diverse fields of engineering mechanics of solids, is a simple splitting test of a disc loaded by a compressive line load generating a tensile stress inside the disc until it fails (Hondros, 1959; Rocco et al, 1999). The idea of the BTS was initiated by a coincidental observation of a church being moved on concert rollers in Brazil, and has been developed gradually since then. It is now widely accepted for indirect measurement of the tensile strength of a given brittle material where the familiar direct tension test (e.g. of a steel bar) is not practical. A state of the art review of the BTS test method, in particular for the testing of rock specimens, can be found in (Diyuan and Louis, 2012). Based on the conventional 2D elastic theory, it is evident that the maximum tensile stress in a Brazilian loaded specimen occurs at its centre with a magnitude of (ISRM, 1978; ASTM, 2008):

$$\sigma_{t,Max} = \frac{P}{2\pi L} \quad (1)$$

where P is the applied compressive load at failure per radius (r_0), assumed to be distributed over an arc length usually less than 15 degrees ($2\alpha \leq 15^\circ$), and $2L$ is the thickness of the disc (see Fig. 1). It is worth mentioning that in the derivation of (1), the distribution of the applied load in the axial (out of plane) direction is assumed uniform, i.e. the disc is under a plane stress condition. Simplicity, ease of sample preparation and reasonable control over the specimen size have made the BTS a very popular method for indirect measurement of the tensile strength of solid-brittle materials.

As an effective method of measuring the tensile strength of a wide range of geo- and construction substances (Hondros, 1959; Wijk, 1978; Kourkoulis et al, 2012), the Brazilian test has also been widely applied to disc specimens

of harder and stiffer polymers, cemented carbides, advanced ceramics and diamond composites (Cranmer and Richerson, 1998; Serati, 2014). However, it has been long reported that following all the test prerequisites of the standard Brazilian method may not be practical with such materials. Deviations from standard recommendations arise mainly from the violation of the accepted boundary conditions in a conventional BTS test method, e.g. the occurrence of non-uniform contact load distributions along the specimen thickness also over the specimen perimeter (Serati, 2014; Hooper, 1971).

The literature is almost replete with analytical works to account for such deviations, in particular to study: (i) the effect of two-dimensional (2D) boundary conditions (Kourkoulis et al, 2012), (ii) the specimen size (Rocco et al, 1999), and (iii) the width of the bearing stripes in the BTS (Rocco et al, 2001). However, the application of a non-uniform pressure along the thickness of the BTS has not yet received adequate attention. This, in return, requires a three-dimensional (3D) theoretical framework to improve and enhance the current 2D solutions. Referring to little research results available on the application of 3D theories relevant to the Brazilian test (Serati et al, 2013; Wei and Chau, 2013), this note aims to study the 3D boundary effect of contact pressure along the axial direction. To pursue the objectives, the analytical recipe presented by Serati et. al (Serati et al, 2013) for the stress analysis of 3D cylinders under arbitrary surface loads is followed due to its ease in introducing a complex boundary condition at contacts using the double Fourier expansion technique.

2 A Non-Uniform Contact Pressure Along the Thickness of the BTS

To check the effect of a non-uniform contact load along the thickness on the Brazilian result, the distribution of the load is assumed parabolic along the z -direction, but uniform on its circumference. The loading is schematically represented in Fig. 2 by green dot lines, where for ease of comparison, the line load (black solid line) and the uniformly distributed radial load (red solid lines) for which Eq. (1) was originally derived, are also illustrated. The double Fourier series expressing the assumed non-uniform thickness loading yields:

$$\begin{aligned} \sigma_{rr}(r=r_0, \theta, z) = & -\frac{P}{\pi \alpha L} \left(\frac{\alpha}{2} + \sum_{m=2,4,6}^{\infty} \frac{\sin(m\alpha)}{m} \cos(m\theta) \right) \\ & \times \frac{3}{2} \left(\sum_{n=1}^{\infty} \frac{8n\pi + 32 \cos(\frac{n\pi}{4}) \sin(\frac{n\pi}{4}) - 16n\pi \cos^2(\frac{n\pi}{4})}{n^3 \pi^3} \cos(\gamma_n z) \right. \\ & \left. + \frac{2}{3} \sum_{n=1}^{\infty} \frac{(1 - \cos(n\pi)) \sin(\frac{n\pi}{2})}{n \pi} \cos(\gamma_n z) \right) \quad (2) \end{aligned}$$

where L is half the thickness of the disc, $\gamma_n = \frac{n\pi}{2L}$, 2α denotes the arc loading angle over which the assumed radial load is applied, and P is the total

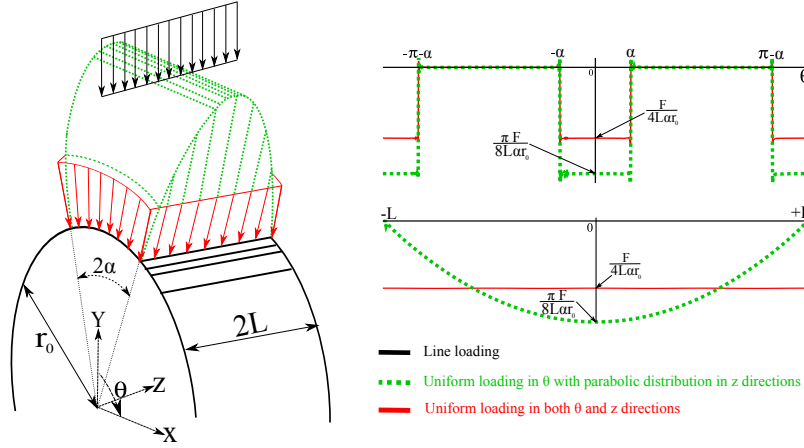


Fig. 2 The loading types comparatively considered

force per radial length (or F/r_0) acting on one side of the disc ($0 \leq \theta \leq \pi$). The characterisation of the parabolic loading introduced in (2) guarantees that

$$r_0 \int_{-L}^L \int_0^\pi \sigma_{rr}(r=r_0) d\theta dz = F \quad (3)$$

To obtain the relevant stress components induced by the pressure in Eq. (2), one needs to first employ the coordinate-independent Papkovitch-Neuber (PN) relation (4) in (r, θ, z) domain following the methodology discussed by Serati et al. (Serati et al, 2013),

$$2\mu \mathbf{u} = -4(1-\nu) \boldsymbol{\psi} + \nabla(\mathbf{R} \cdot \boldsymbol{\psi} + \phi) \quad (4)$$

In Eq. 4, \mathbf{u} is the elastic displacement field, μ is Lamé's constant, ν is Poisson's ratio, \mathbf{R} represents radial position vector in the domain of interest and $\boldsymbol{\psi}$ and ϕ are a harmonic vector ($\nabla^2 \boldsymbol{\psi} = \mathbf{0}$) and a harmonic scalar potential ($\nabla^2 \phi = 0$). The critical step, therefore, is to find general solutions for $\boldsymbol{\psi}$ and ϕ that produce the same boundary Fourier terms as in Eq. (2) after substituting in Eq. (4) at $r = r_0$. To this end, the method of separation of variables can be employed to reduce the resultant PDEs to ODEs (Serati et al, 2013). It follows that ϕ takes the form:

$$\begin{aligned} \phi(r, \theta, z) = & \sum_{n=1}^{\infty} B_{0n} I_0(\gamma_n r) \cos(\gamma_n z) \\ & + \sum_{m=2,4,6}^{\infty} \sum_{n=1}^{\infty} D_{mn} I_m(\gamma_n r) \cos(\gamma_n z) \cos(m\theta) \end{aligned} \quad (5)$$

while the acceptable vector components ψ_r and ψ_θ to satisfy $\nabla^2 \boldsymbol{\psi}(\psi_r, \psi_\theta, 0) = \mathbf{0}$ become:

$$\begin{aligned} \psi_r = & \sum_{n=1}^{\infty} B'_{0n} I_1(\gamma_n r) \cos(\gamma_n z) \\ & + \sum_{m=2,4,6}^{\infty} \sum_{n=1}^{\infty} \left(D'_{mn} I_{m+1}(\gamma_n r) + D''_{mn} I_{m-1}(\gamma_n r) \right) \cos(\gamma_n z) \cos(m\theta) \end{aligned} \quad (6)$$

$$\begin{aligned} \psi_\theta = & \sum_{n=1}^{\infty} B''_{0n} I_1(\gamma_n r) \cos(\gamma_n z) \\ & + \sum_{m=2,4,6}^{\infty} \sum_{n=1}^{\infty} \left(D'_{mn} I_{m+1}(\gamma_n r) - D''_{mn} I_{m-1}(\gamma_n r) \right) \cos(\gamma_n z) \sin(m\theta) \end{aligned} \quad (7)$$

Having known the Fourier form of the presumed applied load as in Eq. (2), one obtains all the constants B_{0n} , B'_{0n} , B''_{0n} , D_{mn} , D'_{mn} , and D''_{mn} for each pair of m and n by substituting (5), (6) and (7) into (4) and comparing the coefficients of each group of terms $\cos(\gamma_n z)$, $\cos(\gamma_n z) \cos(m\theta)$, and $\cos(\gamma_n z) \sin(m\theta)$ with those given from the Fourier boundary conditions in (2). This, for instance, gives $B''_{0n} = 0$ to fulfil the presumed boundary conditions at $r = r_0$. Substituting back the calculated constants into the stress components produced by relation (4), 3D stress components are recovered. It is also of importance to note that other practical boundary conditions at contact, e.g. Hertzian distributions both along the thickness and on the periphery of the disc, can be readily analysed in the same manner once the target distribution is introduced by an appropriate double Fourier series. For example, for the case when the externally imposed radial pressure is considered uniform over the thickness, but varies according to a parabolic law along the contact at the periphery of the disc, the Fourier expansion reads:

$$\begin{aligned} \sigma_{rr}(r=r_0, \theta, z) = & -\frac{2P}{\pi \alpha L} \left(\frac{\alpha}{2} + \sum_{m=2,4,6}^{\infty} \frac{3 \sin(m\alpha) - 3m\alpha \cos(m\alpha)}{m^3 \alpha^2} \cos(m\theta) \right) \\ & \times \sum_{n=1}^{\infty} \frac{(1 - \cos(n\pi)) \sin(\frac{n\pi}{2})}{n\pi} \cos(\gamma_n z) \end{aligned} \quad (8)$$

2.1 Numerical Investigation

Based on the aforementioned methodology and for a standard test geometry of the Brazilian test with $\frac{L}{r_0} = 0.5$ and $2\alpha = 10^\circ$, the variation of the radial stress at the middle section ($z = 0$) is compared in Fig. 3 for two loading cases: (i) a load acting uniformly in the z -direction as widely assumed in the available standards (red solid lines in Fig. 2), and (ii) a non-uniform parabolic contact distribution along the BTS thickness as expressed by Eq. (2). From Fig. 3, it

is evident that the tensile value of the radial stress at the centre ($\sigma_{rr}, r=0, \theta=\frac{\pi}{2}$) is almost one-third of the estimated value by Eq. (1), point A in the figure, when the distribution of the load is parabolic (point B). In other words, the conventional expression (1) overestimates the maximum tensile stress with a factor of around 3 (three).

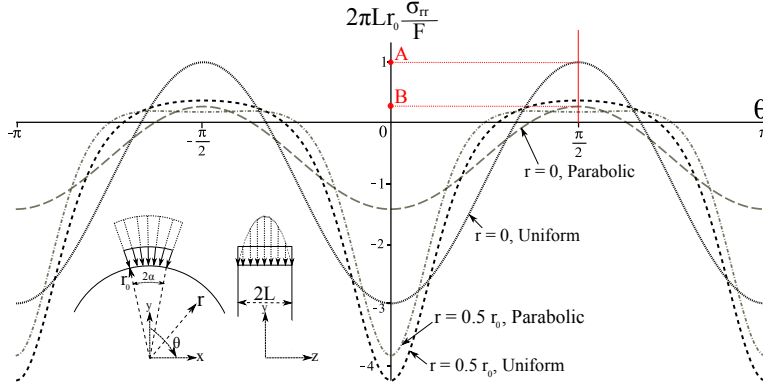


Fig. 3 The effect of parabolic and uniform distribution of loading along the thickness of a standard Brazilian disc with $\frac{L}{r_0} = 0.5$ and $2\alpha = 10^\circ$, when $\nu = 0.25$,

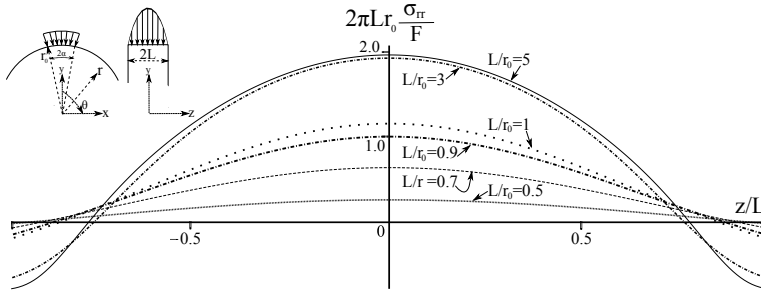


Fig. 4 The variation of radial stress at the centre ($\sigma_{rr}, r=0, \theta=\pi/2$) of a solid disc subjected to parabolic loading along its thickness defined by Eq. (2), when $\nu = 0.25$ and $2\alpha = 10^\circ$

Moreover, the application of a non-uniform load over the thickness of the BTS not only influences the magnitude of the maximum induced tensile stress, but also changes its location within the specimen domain as a function of disc's aspect ratio, or $\frac{L}{r_0}$ (see Figs. 4 and 5,). That is, in thin discs with $\frac{L}{r_0} < 0.7$, the location of the maximum tensile stress is displaced from the disc's centre to the perimeter. Thus, the transition from plane stress to plane strain, i.e. thin disc to cylinder, could greatly change the location and the value of the maximum tensile stress in a Brazilian disc if the contact load along the specimen thickness is not uniform. In other words, for a conventional Brazilian specimen, in which

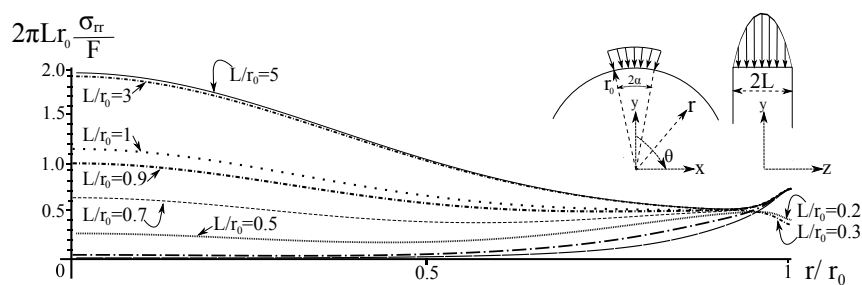


Fig. 5 The variation of tensile stress throughout a disc subjected to the loading defined by (2), when $\nu = 0.25$ and $2\alpha = 10^\circ$

$0.25 \leq \frac{L}{r_0} \leq 0.75$, expression (1) needs to be taken into account with great care if the uncertainty of the load distribution along the thickness is large. Otherwise, an erroneous result is expected as predicted in Figs. 3–5.

3 Conclusion

Using a three-dimensional analytical approach, the sensitivity of the Brazilian test to its standard testing recommendations was investigated. It was concluded that the tensile stress induced in a Brazilian disc is significantly affected by the distribution of the applied load along its thickness rather than its circumferential condition. Under a non-uniform contact pressure along the BTS thickness, it was evident that both the numerical value and the location of the maximum tensile stress varied as a function of the geometrical aspect ratio of the disc specimen. For test conditions in which load distribution in the contact region along the thickness does not follow the standards or the uncertainty of its exact nature is large, e.g. in testing of super hard materials with relatively high stiffness and hardness greater than the contact testing platens, great care should be taken in regard to the interpretation of the Brazilian test result.

References

- ASTM (2008) D3967-08: Standard test method for splitting tensile strength of intact rock core specimens. ASTM International, West Conshohocken, PA, USA, annual Book of ASTM Standards
- Cranmer D, Richerson D (1998) Mechanical testing methodology for ceramic design and reliability. Springer-Verlag, CRC Press
- Diyuan L, Louis NYW (2012) The Brazilian disc test for rock mechanics applications: review and new insights. *Rock Mechanics and Rock Engineering* 46(2):269–287
- Hondros G (1959) The evaluation of Poisson's ratio and the modulus of materials of a low tensile resistance by the Brazilian (indirect tensile) test

- with particular reference to concrete. *Australian Journal of Applied Science* 10:243–268
- Hooper JA (1971) The failure of glass cylinders in diametral compression. *Journal of the Mechanics and Physics of Solids* 19(4):179–200
- ISRM (1978) Suggested methods for determining tensile strength of rock materials. *International Journal of Rock Mechanics and Mining Science & Geomechanics Abstracts* 15(3):99–103
- Kourkoulis SK, Markides CF, Chatzistergos PE (2012) The Brazilian disc under parabolically varying load: Theoretical and experimental study of the displacement field. *International Journal of Solids and Structures* 49(7–8):959–972
- Rocco C, Guinea GV, Planas J, Elices M (1999) Size effect and boundary conditions in the Brazilian test: Theoretical analysis. *Materials and Structures* 32(220):437–444
- Rocco C, Guinea G, Planas J, Elices M (2001) Review of the splitting-test standards from a fracture mechanics point of view. *Cement and concrete research* 3(1):73–82
- Serati M (2014) Stiness and strength of rock cutting and drilling tools and rock–drag bit and roller disc cutters. PhD thesis, School of Civil Engineering, The University of Queensland, Australia
- Serati M, Alehossein H, Williams DJ (2013) 3D elastic solutions for laterally loaded discs: generalised Brazilian and Point Load tests. *Rock Mechanics and Rock Engineering* pp 1–15
- Wei XX, Chau KT (2013) Three dimensional analytical solution for finite circular cylinders subjected to indirect tensile test. *International Journal of Solids and Structures* 50(14–15):2395–2406
- Wijk G (1978) Some new theoretical aspects of indirect measurements of the tensile strength of rocks. *International Journal of Rock Mechanics and Mining Science & Geomechanics Abstracts* 15(4):149–160